Photo-Fenton Oxidative System for Removing Tartrazine Yellow Dye in Aqueous Medium Using Y-fe Zeolite As Catalyst

Ramiro Picoli Nippes (ramiro_picoli@yahoo.com.br)
Universidade Estadual de Maringa https://orcid.org/0000-0002-9919-003X
Paula Derksen Macruz
Universidade Estadual de Maringa
Luiza Carla Augusto Molina
Universidade Estadual de Maringa
Mara Heloísa Neves Olsen Scaliante
Universidade Estadual de Maringa

Research Article

Keywords: H2O2, Photo-Fenton, Tartrazine Yellow, Zeolite, Catalyst, Azo dye

Posted Date: December 14th, 2021

DOI: https://doi.org/10.21203/rs.3.rs-1025314/v1

Abstract

The synthesis and application of heterogeneous solid catalysts in Fenton-type processes have been shown to be a promising alternative for the removal of hazardous pollutants. In this context, the aim of this study was to prepare and characterize a heterogeneous solid iron catalyst supported on zeolite Y for the degradation of yellow food coloring tartrazine (TY). The catalyst was produced through humid ion exchange and characterized by the physisorption of N2, XRD, SEM, TEM and EDX. The efficiency of the catalyst was evaluated through the degradation of tartrazine yellow dye in a batch regime, and the influence of some of the main operational parameters was also evaluated. The characterizations confirmed the presence of iron on the surface of zeolite Y and the increase in the specific area and pore volume after ion exchange. The catalyst used in the photo-Fenton system was extremely efficient, with a removal of approximately 98% in 120 min in the experimental conditions: [TY]0 = 10 mg/L, [H2O2]0 =200 g/L, Y-Fe dosage=1.5 g/L and pH= 3.0. It was possible to recover the catalyst and use it in five reuse cycles, showing its stability and potential application of this catalyst in heterogeneous photo-Fenton systems.

1. Introduction

Advanced oxidative processes (AOP) have recently emerged in the removal from toxic chemicals of aqueous medium, due to their high efficiency, versatility and simplicity, making them an appropriate choice with great potential for application in contaminated wastewater treatment (Tekbaş et al. 2008). These processes are based on the production of powerful reactive species, usually radial, which can target and mineralize almost all oxidizable substances (Thomas et al. 2021).

Among the available technologies, the use of Fenton-type processes has been shown to be an innovative and suitable treatment method for the removal of numerous dangerous pollutants (Rache et al. 2014) in addition to being simple and relatively inexpensive, and it can also occur at low temperatures and atmospheric pressure (Neamţu et al. 2004). The homogeneous Fenton and photo-Fenton processes occur through the reaction between ferrous ions (Fe^{2+}/Fe^{3+}) and hydrogen peroxide, in the presence or absence of UV radiation, respectively, for the production of highly oxidizing hydroxyl radicals (Duarte and Madeira 2010).

However, the main disadvantages of these processes are related to the formation of iron containing sludge and/or the need for recovery of the iron catalyst after treatment (Tekbaş et al. 2008). To overcome this problem, the synthesis and application of heterogeneous Fenton type solid catalysts has been shown to be a promising and efficient alternative. For that, iron ions are adsorbed on the surface of porous materials, allowing the catalysts to react with hydrogen peroxide H_2O_2, generating hydroxyl radicals (·OH) and preventing the loss of Fe species through precipitation in the reaction (Noorjahan et al. 2005).

In this sense, zeolites are considered as a support option for the preparation of heterogeneous Fenton-type catalysts, due to their adsorption and ion-exchange characteristics. Iron-exchanged zeolites have

been shown to be promising catalysts in pollutants oxidation by H_2O_2 with catalytic activities similar to homogeneous iron ions (Neamţu et al. 2004; Amat et al. 2004; Noorjahan et al. 2005; Duarte and Madeira 2010; Rache et al. 2014). Among the available zeolites, zeolite Y has been widely used in the petrochemical, fine chemical and water treatment industries, due to its appreciable characteristics such as high stability and activity. (Yang et al. 2019; Guo et al. 2019).

In this study, the photo-Fenton reaction was evaluated using UV-A radiation and a heterogeneous solid iron catalyst supported on zeolite Y for degradation of the yellow food dye tartrazine (TY). The efficiency of the heterogeneous oxidation process was evaluated by examining the influence of some of the main operating parameters, such as pH, H_2O_2, and catalyst reuse. The chosen contaminant was the TY dye, an azo dye used by the food industry to promote the yellow color in products, and it has a complex aromatic structure and stability, which characterizes it as a dangerous compound for the environment and conventional biological treatment methods are ineffective for its degradation (Souza et al. 2021).

2. Experimental

2.1. Chemicals

Zeolite NaY was kindly provided by CENPES/PETROBRAS. Iron (II) sulfate heptahydrate (FeSO4.7H2O, Sigma Aldrich, 98%). The food dye tartrazine was acquired from Sigma Aldrich and diluted in distilled water to prepare the working solutions.

2.2. Preparation of the catalyst

In this study, a simple and low-cost ion exchange method was employed. 1 g of NaY-zeoilte was suspended in 25 ml of 0.05 M FeSO4 and stirred magnetically for 6 h. The sample was filtered, washed with water and collected after filtration. The material was dried in an oven at 100°C for 24 h. The final product is zeolite Y exchanged with iron, which will be identified as Y-Fe.

2.3. Characterization of samples

The Y-Fe catalyst was characterized through a textural analysis by N_2 physisorption at 77 K performed in a Micromeritics ASAP 2020C equipment. Powder X-ray diffraction (XRD, Shimadzu LabX 6000) using Cu-Kα radiation source at 2θ range of 5 to 60º with a 0,02º stage (40 kv with a 30 mA current). The surface morphologies of the samples were studied using a Shimadzu SS-550 scanning electron microscope (SEM) connected to an energy dispersion spectrometer (EDX), Superscan SS-550, to verify the elemental composition of the sample surfaces, selecting some regions.

2.4. Heterogeneous photo-Fenton oxidation of TY

It is known that the contaminant adsorption process on the catalyst surface plays an important role in its degradation. For this reason, the contribution of this process was evaluated. To this end, the tests were carried out in batch process with 250 ml of aqueous TY solution in contact with 0.37 g of zeolite Y or

zeolite Y-Fe for comparison. After the desired contact time, the adsorbent was recovered from the dye solution by filtration and the concentration of TY remaining in the solution was measured using a UV-vis spectrophotometer (DR-2700 Hach) at its maximum wavelength of 426 nm. The amount of TY adsorbed per unit mass of the adsorbent at equilibrium (q_t, mg/g) was calculated as follows:

$$q_t = \frac{\left(C_0 - C_e\right) . V}{m} \quad (1)$$

Where C_0 and C_e are the initial and equilibrium TY concentrations (mg/L), respectively, V is volume of the TY solution (L) and m is the mass of adsorbent (g).

Bleaching experiments were carried out in batch process on a system isolated from the external environment by an aluminum metal box equipped with two side fans for internal cooling. This reaction system consisted of a glass beaker, with a capacity of 500 ml, equipped with a magnetic stirrer, to improve catalyst dispersion, and five tubular UVA lamps, measuring 26 mm×450 mm, wattage of 45 W, and intensity luminous of 0.061 W m^{-2}.

In each experiment, a concentration of 1.5 g/L of catalyst and solutions of 250 mL of TY diluted at 10 mg/L were used. The pH of the solution was adjusted to the desired value using HCl (0.1 M) or NaOH (0.1 M).

The percentage of process degradation was determined by $((C_o\text{-}C_t)/C_o)\times100$, where C_o and C_t are the initial and the freely dissolved TY concentration, respectively.

3. Results And Discussion

3.1. NaY and Y-Fe catalyst characterization

Table 1 shows the textural parameters of the material samples. According to the results, the NaY zeolite used in this work has a total pore volume of 0.38 cm^3 g^{-1} and a specific area of 724.76 m^2 g^{-1}, which corroborates with the reported data of NaY surface area being generally amongst 400 to 1000 m^2 g^{-1}. It is important to note that the specific area and pore volume of zeolite NaY increased after the ion exchange process, this result is in agreement with other studies in the literature (Xiong et al. 2021; Ba Mohammed et al. 2021).

Table 1
Texture parameters of samples obtained through N_2 physisorption.

Sample	Specific area [m^2 g^{-1}]	Pore size [nm]	Pore volume [cm^3 g^{-1}]
NaY	724.76	1.87	0.38
Y-Fe	840.56	1.93	0.45

The morphology of unexchanged and exchanged zeolites is shown in Fig. 1a and Fig. 1b. It can be noted that the samples have clumps and irregular morphology of different sizes. It is observed that the ion exchange of Na for Fe does not cause noticeable changes in the structure of the NaY zeolite. The TEM image (Fig. 1c) reveals the deposition of iron particles on the surface of the zeolite.

The chemical composition of non-exchanged and exchanged zeolite was performed using the SEM/EDX technique and its results are in Table 2. It is possible to observe that the presence of iron was not detected in the non-exchanged zeolite sample. After the synthesis of the material by ion exchange, it was noted a decrease in the Na content from 10.8–1.8% and the presence of iron content (7.6%), therefore showing that the exchange of Na for Fe was effective. Furthermore, an increase in the O content from 61.4–68.3% can be seen, suggesting that most metals may be present in oxide form.

Table 2
Elemental composition of samples by EDX.

Sample	O	Si	Na	Al	Fe
NaY	61.4	17.2	13.2	8.2	0
Y-Fe	68.3	15.6	1.8	6.7	7.6

The XDR patterns of exchanged and unexchanged zeolites are shown in Fig. 2a. XRD profiles were analyzed using X'Pert HighScore Plus software and compared to ICDD PDF2 database. PDF#00-043-0168 indicates that the peaks of greater intensity at 2 = 6.23º, 15.64º and 23.63º correspond to zeolite Y (Na). After ion exchange synthesis is performed, it is observed the occurrence of crystallinity loss in the sample, which may be related to the charge effect on the ion exchange cation in the zeolitic structure (Rache et al. 2014). The XRD profile of the exchanged zeolite shows peaks associated with iron oxide structures (hematite Fe_2O_3) that are not identified in the unexchanged zeolite. Three new peaks are identified according to PDF#00-001-1053 at 2 = 33.14º, 35.71º and 54.04º. The presence of these peaks, even at a relatively low intensity, indicates that part of the exchanged iron was incorporated into the zeolite crystal structure.

3.2. Adsorption process

From the adsorption experiments, in batch regime, it was possible to evaluate the adsorptive capacity of the materials used in the removal of TY dye in aqueous medium. The results obtained at room temperature are shown in Fig. 3. through the contact time (min) versus the adsorbed amount (mg g^{-1}).

When evaluating the results, it is possible to observe the behavior of the adsorption process, which can be divided into two moments; the first refers to a more significant adsorption of the dye up to approximately 75 min of adsorption, due to the greater availability of sites on the surface of the materials (Liu et al. 2021). After this first stage, the adsorption gradually weakened, leading the process to an equilibrium state, because of the scarcity of adsorption sites and the excessively rare concentration of TY dye molecules in the medium (Ba Mohammed et al. 2020). The maximum adsorbed amount of dye was from 1.04 to 1.51 mg g^{-1} using NaY and Y-Fe respectively. This small increase in adsorption is related to the increase in the values of the textural parameters of zeolite Y, such as the specific area and pore volume, promoted by the presence of iron on the material surface (Omri et al. 2020; Kang et al. 2021). This increase in adsorption capacity is important for the efficiency of advanced oxidative processes, such because photo-Fenton, as it generates a synergistic effect between the processes already reported in the literature (Zhao et al. 2020).

3.3. Decolorization process of TY dye in different systems

Figure 4 shows the TY dye decolorization efficiency (%Removal) as a function of time (min) in each system. Assessing the results of the reactions, it is possible to state that H_2O_2 alone was unable to generate substantial discoloration of TY, about 13% after 120 min of reaction, which can be explained by the low generation of oxidizing species, such as hydroxyl radicals, which are the main species responsible for promoting the discoloration of the solution (Valéria da Fonseca Araujo et al. 2006; Omri et al. 2020), this result corroborates with the study by Fragoso et al., 2009 (Fragoso et al. 2009), that evaluated the degradation of C.I. Food Yellow 4 azo dyes by the oxidation with hydrogen peroxide. When UV-A radiation was introduced into the system together with H_2O_2, the TY discoloration increased to approximately 50% at the end of the reaction time. This increase was due to direct photolysis of H_2O_2 by UV-A radiation, which promotes the generation of hydroxyl radicals from the decomposition of H_2O_2 during photochemical reactions (Hernández-Oloño et al. 2021). A similar result was observed for the system formed by the solid catalyst Y-Fe and UV-A radiation that showed a dye discoloration of approximately 46%. This result is associated with the optical property of iron, which has a band gap energy value around 2.2 eV (Balu et al. 2019) that guarantees the ability to absorb light in the visible region (>400 nm) and high catalytic activity, as expected (Kumar et al. 2013; Nezamzadeh-Ejhieh and Shahriari 2014).

Regarding the process widely known as Fenton (Y-Fe + H_2O_2), it is possible to verify a significant and desirable efficiency of about 80% discoloration after 120 min of reaction. This result is due to the success of the Fenton oxidation reaction, in which the iron supported on the zeolite played the role of catalyst for the catalytic decomposition of the H_2O_2 present in solution, promoting the generation of hydroxyl radicals OH with high oxidative power (Tekbaş et al. 2008; Shin et al. 2021).

Finally, the heterogeneous photo-Fenton process (Y-Fe + H_2O_2 + UV-A) resulted in an extremely efficient decolorization, 80% within 30 min of process, and 98.34% after 120 min. In this system, the rapid discoloration of the TY dye solution is a result of the formation of the photo-Fenton oxidative system,

which promotes the oxidation of TY molecules, through the efficiency of the species involved in the process, as observed in previous systems. In this system, the formation of OH radicals is continuously generated by the action of UV-A radiation, which helps in the dissociation of H_2O_2 and also promotes the photolysis of iron ions, reducing the initial oxidation number, that reacts with H_2O_2, catalyzing the formation of oxidizing species (Oancea and Meltzer 2013; Palas et al. 2017). The reactions results prove that the solid catalyst, produced in this study, was efficient in removing the yellow azo dye tartrazine and showed to be adequate for the realization of the Fenton and photo-Fenton oxidative systems.

3.4. Influence of H_2O_2 concentration

Hydrogen peroxide performs an important role in Fenton photo-type oxidation systems as an oxidizer and main source of hydroxyl radicals (Palas et al. 2017; Dhawle et al. 2021). The effect of H_2O_2 concentration on the TY dye removal process was evaluated using H_2O_2 concentrations between 100-400 mg L^{-1}. The results are shown in Fig. 5, where it is possible to see that, in general, the increase in H_2O_2 concentration did not change the final result of TY discoloration; however, there was an increase in the speed of the photo-Fenton reaction as can be seen in the first 15 min of the process. This can be explained by the greater availability of hydroxyl radicals in the medium that potentiates TY discoloration, indicating that the break of H_2O_2 through photolysis was completed during this period (Crittenden et al. 1999; Ramos et al. 2020). However, after this first moment, the oxidation process stabilizes, this may be related to the excess of H_2O_2, which can act as a hydroxyl radical scavenger, forming the hydroperoxyl radical that has less reduction potential than •OH, therefore harming the degradation process (Paterlini and Nogueira 2005). Elmorsi et al. 2010 warns that the concentration of H_2O_2 can increase or inhibit the photoreaction rate depending on the concentration. Therefore, an optimal concentration of H_2O_2 in the course of the reaction must be achieved.

3.5. Influence of the solution initial pH

The pH influence on the decolorization efficiency of TY dye was evaluated using pH range from 2 to the solution natural pH (8.2-8.5). The result is shown in Fig. 6. Analyzing the data, it is possible to verify that the test at pH 02 provides an accelerated discoloration with almost 80% removal in just 15 min. However, after this period of time, the efficiency stabilizes and becomes lower than that performed at pH 03. According to the literature, this effect is associated with the presence of protons in the medium, which can be a scavenger of OH radicals under highly acidic conditions, thus inhibiting the degradation process of the contaminant [31–33]. With the increase of pH to 6 and free pH, the TY degradation process was obviously inhibited, as at higher pH the H_2O_2 quickly decomposes into molecular oxygen and H_2O, but does not transform into hydroxyl radicals, losing its oxidizing capacity (Xia et al. 2011). It is also known that at alkaline pH, as in the TY solution at free pH, iron ions precipitate in the form of $Fe(OH)_2$, reducing process efficiency (Pinheiro et al. 2020). The result obtained reinforces the need for acidification of the solution to the initial pH range considered ideal (2.5-3.0) for photo-Fenton processes (Jiang et al. 2019; Nippes et al. 2021).

3.6. Regeneration and reuse of catalyst

To assess the stability and reuse of the Y-Fe catalyst, reuse tests were carried out. The catalyst was used in six consecutive experiments using fresh dye solutions. After each experiment, the Y-Fe catalyst was removed by vacuum filtration, washed with deionized water several times and oven dried at 60°C for 24 hours.

The results of the reaction cycles are shown in Fig. 7. In which it is possible to state that the catalyst used had excellent stability and great possibility of reuse, with low performance reduction at each reuse and remaining its high catalytic performance. Only the last reuse has a greater reduction in the percentage of discoloration, yet still with removal above 80%. This slight loss of catalytic activity is justified by the loss of catalyst mass in the recycling and leaching process of active materials; however, this is a reasonable phenomenon during the stability test (Qin et al. 2021). To assess the leaching of iron in the solution, we used the atomic absorption spectroscopy technique, performed in a Varian atomic absorption spectrometer, model 50B, with chemical decomposition of the samples, in which no iron element was detected in the solution after the process. This result reinforces the fact that the Y-Fe catalyst has good stability and reusability in heterogeneous photo-Fenton degradation of the TY dye. Furthermore, NaY zeolite can be considered a good support for the formation of solid catalysts for photo-Fenton reaction.

4. Conclusion

A heterogeneous photo-Fenton catalyst was synthesized by a simple humid ion exchange method. The characterization techniques utilized showed that iron species replaced sodium species in the composite and that there was a desired increase in specific area and pore volume. Degradation of yellow food coloring tartrazine was practically total after 120 minutes of photo-Fenton system with constant UV-A radiation, use of hydrogen peroxide and acidic pH. The regeneration and reuse of solid catalyst was evaluated and showed good efficiency during six reaction cycles. Ultimately, it can be expected that this catalyst exerts good photocatalytic activity on an industrial scale for the degradation of food dyes.

Declarations

Ethics approval and consent to participate

Not applicable

Consent for publication

Not applicable

Availability of data and materials

All data generated or analysed during this study are included in this published article.

Competing interests

The authors declare that they have no competing interests.

Funding

The authors would like to thank the Araucaria Foundation (FA-PR) for the RENEWABLE HYDROCARBON (NAPPI-HCR) project for granting a scholarship.

Authors' contributions

Ramiro Picoli Nippes: Conceptualization, Methodology, Investigation, Writing – original draft. Luiza Carla Augusto Molina: Adsorption experiments. Paula Derksen Macruz: Investigation, Writing – original draft, review and editing. Mara Heloísa Neves Olsen Scaliante: Supervision, Writing – review and editing.

References

1. Ahmed B, Limem E, Abdel-Wahab A, Nasr B (2011) Photo-Fenton Treatment of Actual Agro-Industrial Wastewaters. Ind Eng Chem Res 50:6673–6680. https://doi.org/10.1021/IE200266D
2. Amat AM, Arques A, Bossmann SH et al (2004) Oxidative degradation of 2,4-xylidine by photosensitization with 2,4,6-triphenylpyrylium: homogeneous and heterogeneous catalysis. Chemosphere 57:1123–1130. https://doi.org/10.1016/j.chemosphere.2004.08.029
3. Ba Mohammed B, Hsini A, Abdellaoui Y et al (2020) Fe-ZSM-5 zeolite for efficient removal of basic Fuchsin dye from aqueous solutions: Synthesis, characterization and adsorption process optimization using BBD-RSM modeling. J Environ Chem Eng 8:104419. https://doi.org/10.1016/J.JECE.2020.104419
4. Ba Mohammed B, Yamni K, Tijani N et al (2021) Enhanced removal efficiency of NaY zeolite toward phenol from aqueous solution by modification with nickel (Ni-NaY). J Saudi Chem Soc 25:101224. https://doi.org/10.1016/J.JSCS.2021.101224
5. Balu S, Velmurugan S, Palanisamy S et al (2019) Synthesis of α-Fe2O3 decorated g-C3N4/ZnO ternary Z-scheme photocatalyst for degradation of tartrazine dye in aqueous media. J Taiwan Inst Chem Eng 99:258–267. https://doi.org/10.1016/J.JTICE.2019.03.011
6. Crittenden JC, Hu S, Hand DW, Green SA (1999) A kinetic model for H2O2/UV process in a completely mixed batch reactor. Water Res 33:2315–2328. https://doi.org/10.1016/S0043-1354(98)00448-5
7. Dhawle R, Frontistis Z, Mantzavinos D, Lianos P (2021) Production of hydrogen peroxide with a photocatalytic fuel cell and its application to UV/H2O2 degradation of dyes. Chem Eng J Adv

6:100109. https://doi.org/10.1016/J.CEJA.2021.100109

8. Duarte F, Madeira LM (2010) Fenton- and Photo-Fenton-Like Degradation of a Textile Dye by Heterogeneous Processes with Fe/ZSM-5 Zeolite. Sep Sci Technol 45:1512–1520. https://doi.org/10.1080/01496395.2010.487452
9. Elmorsi TM, Riyad YM, Mohamed ZH, Abd El Bary HMH (2010) Decolorization of Mordant red 73 azo dye in water using H2O2/UV and photo-Fenton treatment. J Hazard Mater 174:352–358. https://doi.org/10.1016/J.JHAZMAT.2009.09.057
10. Fragoso CT, Battisti R, Miranda C, de Jesus PC (2009) Kinetic of the degradation of C.I. Food Yellow 3 and C.I. Food Yellow 4 azo dyes by the oxidation with hydrogen peroxide. J Mol Catal A Chem 301:93–97. https://doi.org/10.1016/J.MOLCATA.2008.11.014
11. Guo Q, Li G, Liu D, Wei Y (2019) Synthesis of zeolite Y promoted by Fenton's reagent and its application in photo-Fenton-like oxidation of phenol. Solid State Sci 91:89–95. https://doi.org/10.1016/J.SOLIDSTATESCIENCES.2019.03.016
12. Guo Q, Zhu W, Yang D et al (2021) A green solar photo-Fenton process for the degradation of carbamazepine using natural pyrite and organic acid with in-situ generated H2O2. Sci Total Environ 784:147187. https://doi.org/10.1016/J.SCITOTENV.2021.147187
13. Hassan H, Hameed BH (2011) Fe-clay as effective heterogeneous Fenton catalyst for the decolorization of Reactive Blue 4. Chem Eng J 171:912–918. https://doi.org/10.1016/j.cej.2011.04.040
14. Hernández-Oloño JT, Infantes-Molina A, Vargas-Hernández D et al (2021) A novel heterogeneous photo-Fenton Fe/Al2O3 catalyst for dye degradation. J Photochem Photobiol A Chem 421:113529. https://doi.org/10.1016/J.JPHOTOCHEM.2021.113529
15. Jiang Z, Wang L, Lei J et al (2019) Photo-Fenton degradation of phenol by CdS/rGO/Fe2+ at natural pH with in situ-generated H2O2. Appl Catal B Environ 241:367–374. https://doi.org/10.1016/J.APCATB.2018.09.049
16. Kang JK, Seo EJ, Lee CG, Park SJ (2021) Fe-loaded biochar obtained from food waste for enhanced phosphate adsorption and its adsorption mechanism study via spectroscopic and experimental approach. J Environ Chem Eng 9:105751. https://doi.org/10.1016/J.JECE.2021.105751
17. Kumar S, Kumar B, Baruah A, Shanker V (2013) Synthesis of Magnetically Separable and Recyclable g-C 3 N 4 –Fe 3 O 4 Hybrid Nanocomposites with Enhanced Photocatalytic Performance under. https://doi.org/10.1021/jp409651g. Visible-Light Irradiation
18. Liu J, Lin H, Dong Y et al (2021) The effective adsorption of tetracycline onto MoS2@Zeolite-5: Adsorption behavior and interfacial mechanism. J Environ Chem Eng 9:105912. https://doi.org/10.1016/J.JECE.2021.105912
19. Neamţu M, Zaharia C, Catrinescu C et al (2004) Fe-exchanged Y zeolite as catalyst for wet peroxide oxidation of reactive azo dye Procion Marine H-EXL. Appl Catal B Environ 48:287–294. https://doi.org/10.1016/j.apcatb.2003.11.005

20. Nezamzadeh-Ejhieh A, Shahriari E (2014) Photocatalytic decolorization of methyl green using Fe(II)-o-phenanthroline as supported onto zeolite Y. J Ind Eng Chem 20:2719–2726. https://doi.org/10.1016/j.jiec.2013.10.060
21. Nippes RP, Macruz PD, Neves Olsen Scaliante MH (2021) Toxicity reduction of persistent pollutants through the photo-fenton process and radiation/H2O2 using different sources of radiation and neutral pH. J Environ Manage 289:112500. https://doi.org/10.1016/j.jenvman.2021.112500
22. Noorjahan M, Durga Kumari V, Subrahmanyam M, Panda L (2005) Immobilized Fe(III)-HY: an efficient and stable photo-Fenton catalyst. Appl Catal B Environ 57:291–298. https://doi.org/10.1016/J.APCATB.2004.11.006
23. Oancea P, Meltzer V (2013) Photo-Fenton process for the degradation of Tartrazine (E102) in aqueous medium. J Taiwan Inst Chem Eng 44:990–994. https://doi.org/10.1016/J.JTICE.2013.03.014
24. Omri A, Hamza W, Benzina M (2020) Photo-Fenton oxidation and mineralization of methyl orange using Fe-sand as effective heterogeneous catalyst. J Photochem Photobiol A Chem 393:112444. https://doi.org/10.1016/J.JPHOTOCHEM.2020.112444
25. Palas B, Ersöz G, Atalay S (2017) Photo Fenton-like oxidation of Tartrazine under visible and UV light irradiation in the presence of LaCuO3 perovskite catalyst. Process Saf Environ Prot 111:270–282. https://doi.org/10.1016/j.psep.2017.07.022
26. Paterlini WC, Nogueira RFP (2005) Multivariate analysis of photo-Fenton degradation of the herbicides tebuthiuron, diuron and 2,4-D. Chemosphere 58:1107–1116. https://doi.org/10.1016/j.chemosphere.2004.09.068
27. Pinheiro ACN, Bernardino TS, Junior FEB et al (2020) Enhanced electrodegradation of the Sunset Yellow dye in acid media by heterogeneous Photoelectro-Fenton process using Fe3O4 nanoparticles as a catalyst. J Environ Chem Eng 8:103621. https://doi.org/10.1016/J.JECE.2019.103621
28. Qin H, Yang Y, Shi W et al (2021) Heterogeneous Fenton degradation of azithromycin antibiotic in water catalyzed by amino/thiol-functionalized MnFe2O4 magnetic nanocatalysts. J Environ Chem Eng 9:106184. https://doi.org/10.1016/j.jece.2021.106184
29. Rache ML, García AR, Zea HR et al (2014) Azo-dye orange II degradation by the heterogeneous Fenton-like process using a zeolite Y-Fe catalyst—Kinetics with a model based on the Fermi's equation. Appl Catal B Environ 146:192–200. https://doi.org/10.1016/J.APCATB.2013.04.028
30. Ramos RO, Albuquerque MVC, Lopes WS et al (2020) Degradation of indigo carmine by photo-Fenton, Fenton, H2O2/UV-C and direct UV-C: Comparison of pathways, products and kinetics. J Water Process Eng 37:101535. https://doi.org/10.1016/J.JWPE.2020.101535
31. Shin J, Bae S, Chon K (2021) Fenton oxidation of synthetic food dyes by Fe-embedded coffee biochar catalysts prepared at different pyrolysis temperatures: A mechanism study. Chem Eng J 421:129943. https://doi.org/10.1016/J.CEJ.2021.129943
32. Souza IPAF, Crespo LHS, Spessato L et al (2021) Optimization of thermal conditions of sol-gel method for synthesis of TiO2 using RSM and its influence on photodegradation of tartrazine yellow

dye. J Environ Chem Eng 9:104753. https://doi.org/10.1016/J.JECE.2020.104753

33. Tekbaş M, Yatmaz HC, Bektaş N (2008) Heterogeneous photo-Fenton oxidation of reactive azo dye solutions using iron exchanged zeolite as a catalyst. Microporous Mesoporous Mater 115:594–602. https://doi.org/10.1016/J.MICROMESO.2008.03.001
34. Thomas N, Dionysiou DD, Pillai SC (2021) Heterogeneous Fenton catalysts: A review of recent advances. J Hazard Mater 404:124082. https://doi.org/10.1016/J.JHAZMAT.2020.124082
35. Valéria da Fonseca, Araujo F, Yokoyama L, Alberto César Teixeira L (2006) REMOÇÃO DE COR EM SOLUÇÕES DE CORANTES REATIVOS POR OXIDAÇÃO COM H 2 O 2 /UV. Quim Nov 29:11–14
36. Xia M, Long M, Yang Y et al (2011) A highly active bimetallic oxides catalyst supported on Al-containing MCM-41 for Fenton oxidation of phenol solution. Appl Catal B Environ 110:118–125. https://doi.org/10.1016/J.APCATB.2011.08.033
37. Xiong P, He P, Qu Y et al (2021) The adsorption properties of NaY zeolite for separation of ethylene glycol and 1,2-butanediol: Experiment and molecular modelling. Green Energy Environ 6:102–113. https://doi.org/10.1016/J.GEE.2019.12.006
38. Yang X, Cheng X, Elzatahry AA et al (2019) Recyclable Fenton-like catalyst based on zeolite Y supported ultrafine, highly-dispersed Fe2O3 nanoparticles for removal of organics under mild conditions. Chinese Chem Lett 30:324–330. https://doi.org/10.1016/J.CCLET.2018.06.026
39. Zhao Y, Kang S, Qin L et al (2020) Self-assembled gels of Fe-chitosan/montmorillonite nanosheets: Dye degradation by the synergistic effect of adsorption and photo-Fenton reaction. Chem Eng J 379:122322. https://doi.org/10.1016/J.CEJ.2019.122322

Figures

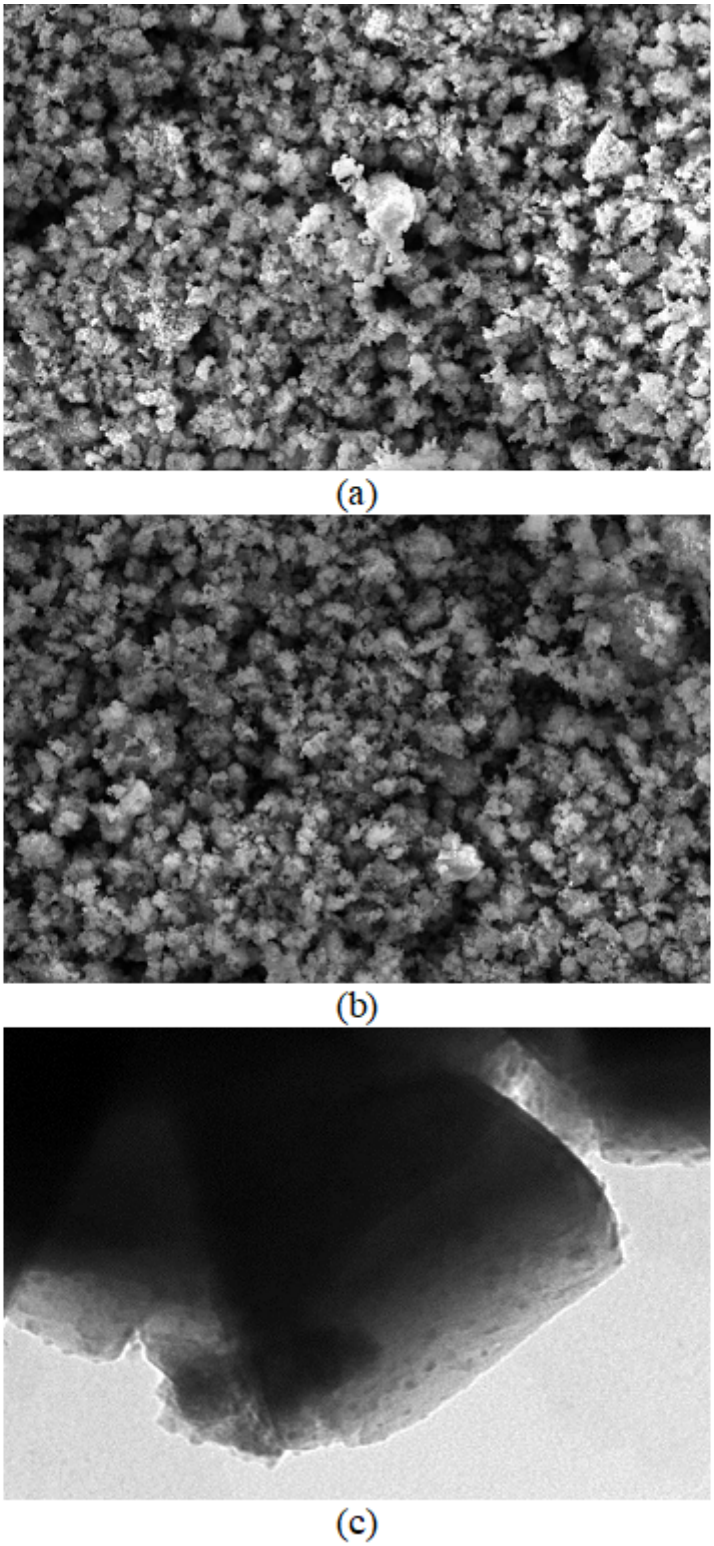

Figure 1

SEM images of (a) Zeolite NaY and (b) Zeolite functionalized with iron FeY, (c) TEM image of Zeolite functionalized with iron FeY.

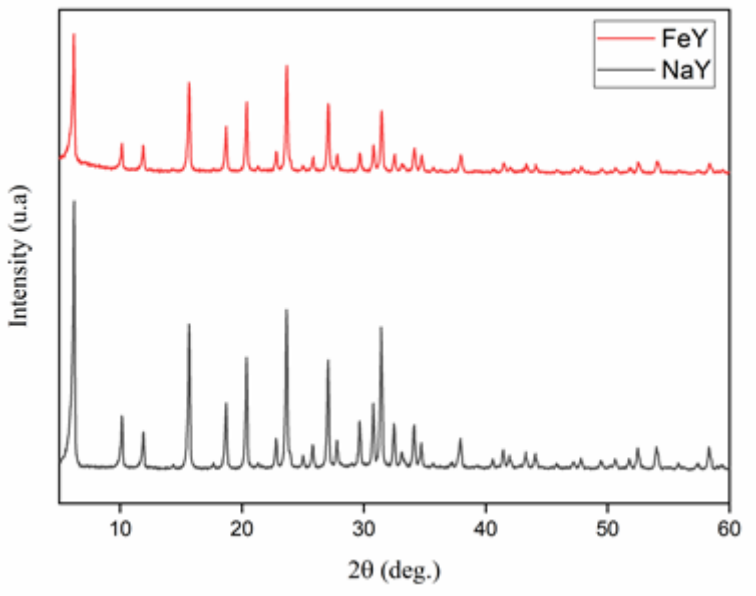

Figure 2

XRD patterns of Zeolite NaY and Zeolite functionalized with iron Y-Fe.

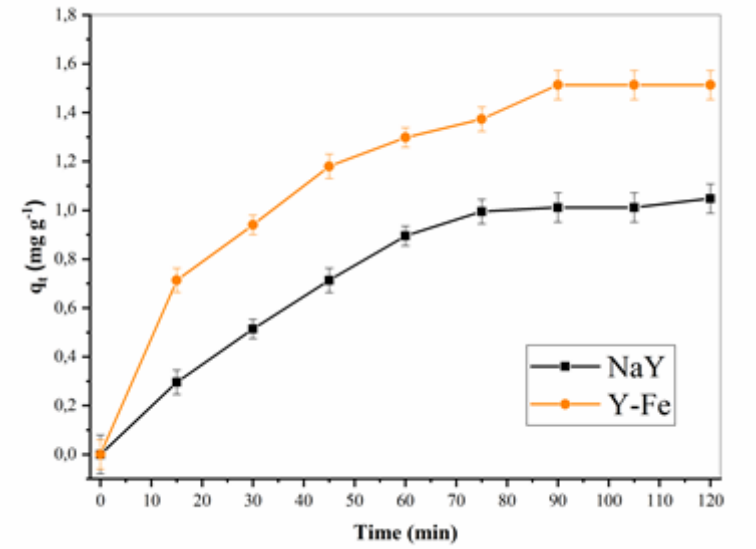

Figure 3

Adsorbed amount of TY (mg g-1) onto NaY and Y-Fe. (Operational parameters: initial concentration of TY [TY]0 = 10 mg/L, adsorbent dosage =1.5 g/L, pH = 3.0).

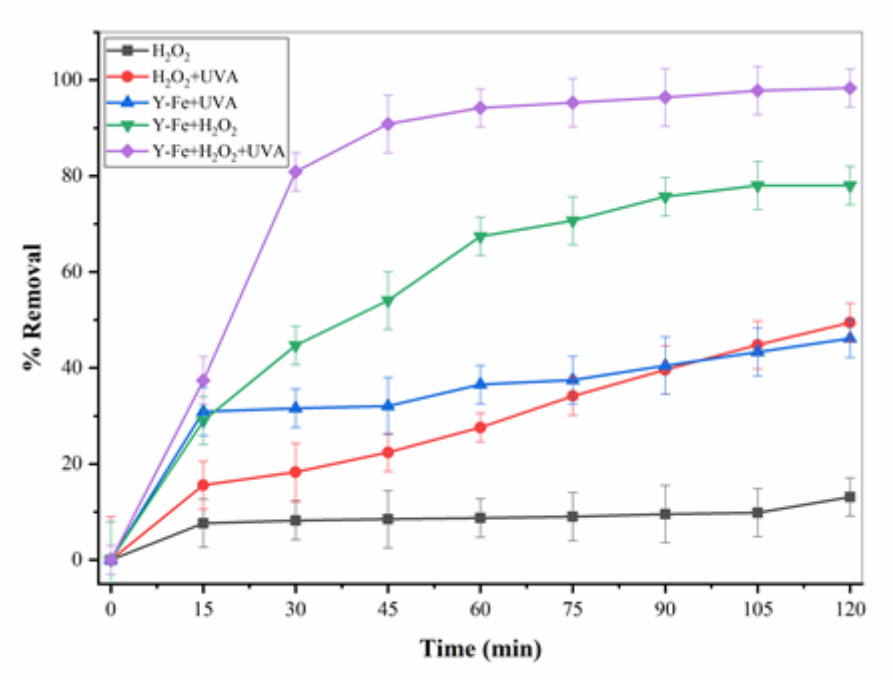

Figure 4

Discoloration of TY in different systems. (Operational parameters: initial concentration of TY [TY]0 = 10 mg/L, initial concentration of H2O2, [H2O2]0 = 200 g/L, Y-Fe dosage = 1.5 g/L, pH = 3.0).

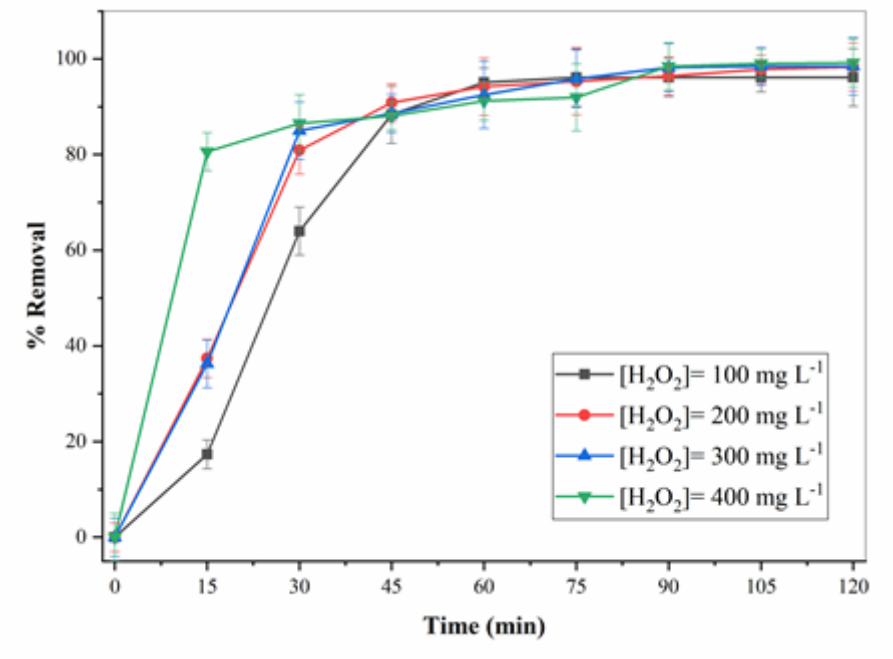

Figure 5

Effect of initial H2O2 concentration on TY discoloration. (Operational parameters: initial concentration of TY [TY]0 = 10 mg/L, Y-Fe dosage = 1.5 g/L, pH = 3.0).

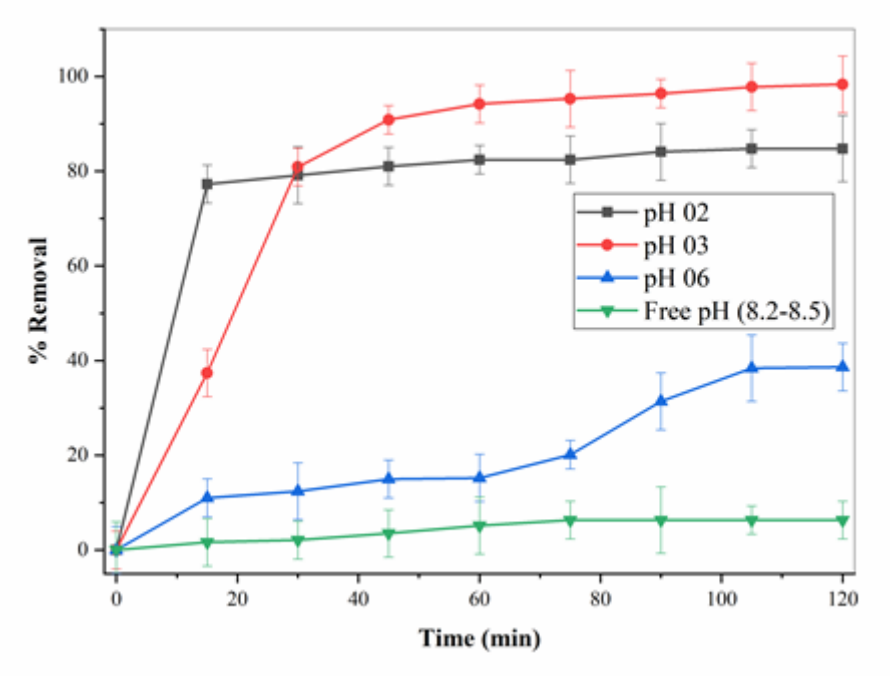

Figure 6

Influence of solution pH on the discoloration efficiency of TY (Operational parameters: initial concentration of TY [TY]0 = 10 mg/L, [H2O2]0 = 200 mg/L, Y-Fe dosage =1.5 g/L).

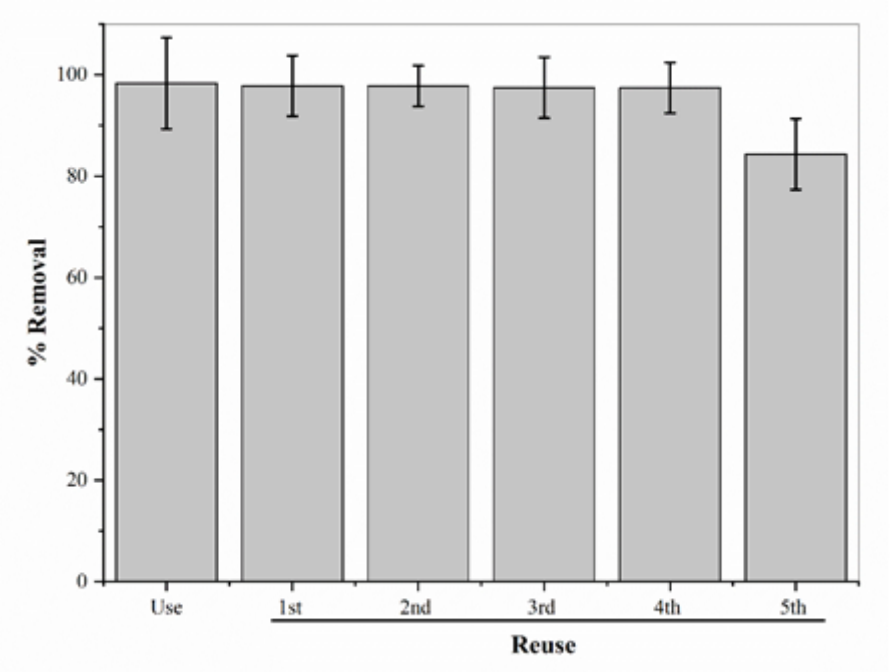

Figure 7

Reuse of catalysts Y-Fe (Operational parameters: initial concentration of TY [TY]0 = 10 mg/L, [H2O2]0 = 200 mg/L, Y-Fe dosage =1.5 g/L).